Dielectric Properties of thin Film $Al/Sb_2Pb_1Se_7/Al$ Devices

Shaila Wagle and Vinay Shirodkar
Solid State Electronics Laboratory, Department of Physics,
The Institute of Science, 15 Madam Cama Road,
Mumhai - 400 032, India

Received 20 January, 2000. Revised version received on 9 May, 2000

Metal - glass metal, MGM, thin film devices are prepared using vacuum deposition of $Sb_2Pb_1Se_7$ compound. The capacitance and the loss tangent variation as a function of temperature and frequency is studied. The observed characteristics are explained using small signal ac circuit analysis. It is shown that the theoretical curve generated using the ac circuit analysis gives excellent fitting with the experimental curve.

I Introduction

Semiconducting glasses, particularly chalcogenides have been widely studied owing to their interesting switching property [1]. These materials are used to fabricate a variety of electronic devices, which arises when the material is cast in thin film form. It is observed that most physical properties reported on chalcogenides have been investigated using polycrystalline pellets or electrodeposits [2,3]. A good amount of work on dc conduction [4], contact capacitance [5], spectral properties [6], ac conduction [7], structural and magnetic properties [8] has been reported by many researchers. However, the dielectric behaviour, such as, variation of capacitance and dielectric loss as a function of temperature and frequency has been overlooked to an extent.

In semiconductor thin film planner integrated circuits, for which high capacity in small space is required, the capacitors may be grown by using either evaporation or sputtering technique. To use the material in thin film circuits it is necessary that the dielectric loss, tan δ, should be in a proper range. However the majority of requirements do not need the lowest tan δ (1% is quite sufficient). But in some cases, like active filters, tan δ should not be more than 0.01%. The aging and temperature variation of capacitance is also important for the material. The temperature coefficient of a capacitance is an important practical parameter for assessing the expected behaviour of a thin film. This malces it necessary to study the effect of temperature and frequency on the device capacitance.

The dielectric behaviour of thin film devices depends not only on their material properties, but also on the substrate used for fabrication and the type of the metal electrodes. Fringing effects at the edges of thin film dielectrics is usually negligible because the thickness of the dielectric is usually very small compare to its lateral dimentions. The magnitude of geometric and measured capacitance may differ if the electric field at the metal insulator interface varies with the insulator over the region. For the given material the film thickness alone establishes the capacitance density which in turns can be used to determine the area needed for a particular capacitance value.

The dielectric loss, which is the part of the energy of an electric field dissipated irrecoverably as heat in dielectric, is comprised of two parts, the first part, which arises due to lead resistance and electrode resistance is frequency dependent and influenced at higher frequencies. This can be minimized using the electrodes of highly conducting metal. The other term is a property of the material itself, which is frequency dependent [9]. Also, the dielectric strength is found to reduce rapidly below about 100nm, owing to pinholes and descret defects in the film.

To the best of our knowledge no report is available on the study of dielectric properties of $Sb_2Pb_1Se_7$ compound. We attempt to report, in this paper, some of the dielectric properties of vacuum deposited $Al/Sb_2Pb_1Se_7/Al$ devices. In all the devices used for the study the thickness of the dielectric film was kept at least above 100nm to minimize the inherent descret defects and pinholes. Also, aluminium was used as an electrode material and its thickness was always maintained above 500nm to reduce lead resistance.

II Experimental

The chalcogenide compound, $Sb_2Pb_1Se_7$, used to fabricate the metal - glass - metal, MGM. devices was prepared by melt quenching. The MGM devices were fabricated on thoroughly cleaned microscope glass slides, using Edwards Co. (UK) Turbomolecular pumping station. The working chamber was fitted with Maxtek (USA) film deposition controller model FDC 440. The base plate housed an eight source turret, while the top plate was fitted with mask changer assembly, both of which could be monitored externally without requiring to break the vacuum. The ultimate working pressure during the deposition was 5×10^{-6} mbar.

Initially, aluminium metal was evaporated to deposit on the substrate in the form of two parallel strips each of 60mm in length, 2mm in width and separated by 5mm from one another. These strips formed the lower electrodes. The material was then deposited through appropriate mask to cover an area of 50mm × 15mm, leaving 5mm of the end portions on both the sides of each aluminium strip. Six counter electrodes, each 2mm wide and 20mm long, perpendicular to the lower electrodes were deposited on the material to obtain 12 MGM devices each of area $4mm^2$ (see Figs. 1a and 1b). The entire deposition sequence was completed without breaking the vacuum at any stage. Fabrication of twelve devices on a single substrate allowed to repeatedly carry out all the electrical measurements on a film, of any particular thickness, prepared essentially under identical deposition conditions.

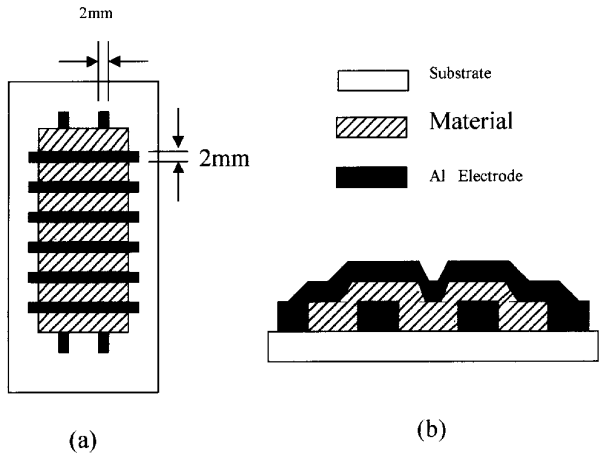

Figure 1. (a) Schematic view of metal - glass - metal devices. (b) Cross sectional view of the devices.

The electrical measurements on the devices were carried out in vacuum using a cryostat, which could be evacuated to 10^{-2} mbar pressure during the measurements. The substrate temperature inside the cryostat could be varied from 150K to 500K. The dielectric measurements were carried using 'Precision LCR Meter' HP model 4284A which could measure and display thirteen different parameters such as capacitance, dielectric loss etc., for different frequencies ranging from 20Hz to 1MHz

III Results

Fig. 2 shows the capacitance-temperature (C - T) characteristics of a typical representative sample with film thickness 270nm. The measurements were carried at 1KHz fixed applied frequency. It is seen that as temperature increases the capacitance also increases in the range of the temperature used for the study. During the sample cooling, the C - T curve traces slightly different path for the first heating and cooling cycle. However, during the subsequent heating and cooling cycles, the C - T curve assumes identical path. All the ac characteristics reported in this paper are based on the measurements carried out on the samples, which were subjected to the thermal cycling as described above.

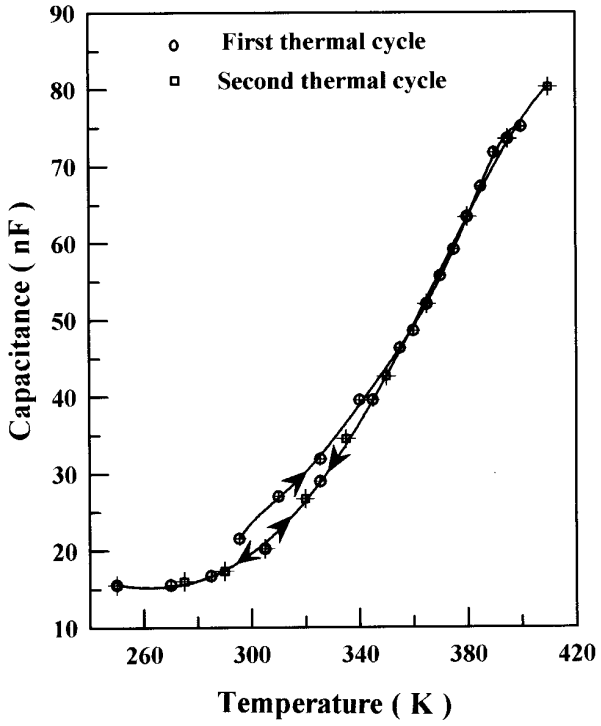

Figure 2. Capacitance - temperature characteristics of the device with film thickness 270nm for 1KHz fixed applied frequency.

Fig. 3 shows a capacitance versus frequency plot of the devices with different film thicknesses at 295K. It is seen that the capacitance initially falls sharply as the frequency increases and then saturates to some value as the frequency approaches 1MHz. The ratio of low frequency to high frequency capacitance obtained from the curves is found to be close to 12:1 for all the film devices. Fig. 4 shows the tan $\delta - \omega$ characteristics of the devices with different film thicknesses at 295K. It is found that tan δ initially decrease with increase in fre-

quency, attains a minimum, and again starts to increase further frequency is increased.

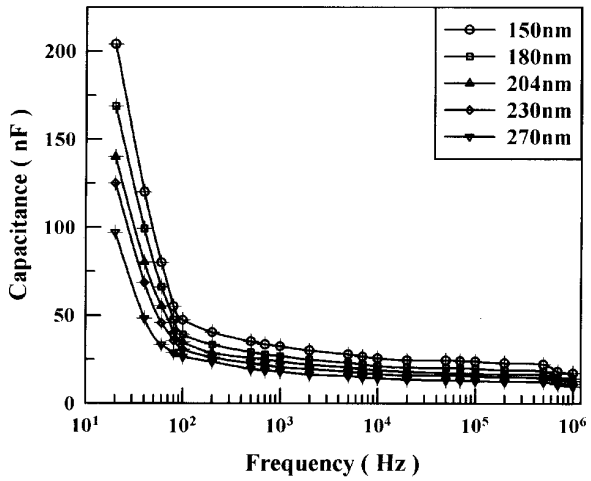

Figure 3. Capacitance versus frequency plots of the devices with different film thickness at 295K.

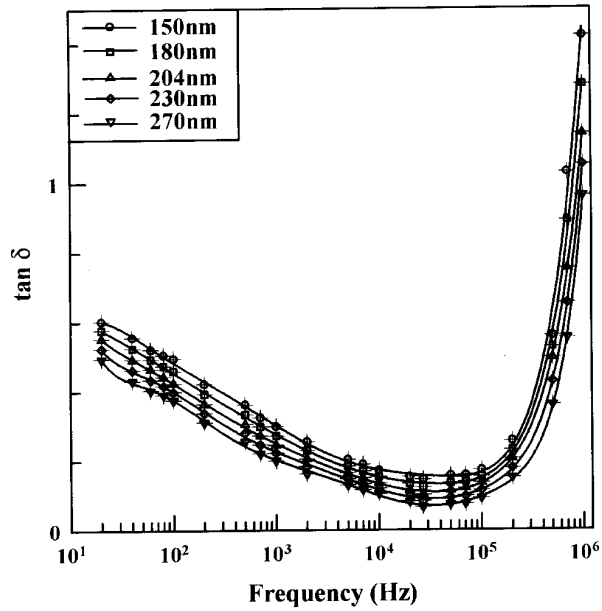

Figure 4. Tan δ versus frequency curves of the devices with different film thicknesses at 295K.

Fig. 5 shows the C - T characteristics of the devices of different film thicknesses at fixed applied frequency of 1KHz. Here the temperatures range chosen for the display of C - T characteristics is 250 to 410K. This is because the capacitance is found to saturate near about 250K and the glass transition temperature, T_g, is found to be 419K from the earlier studies [10]. Fig. 6 shows the C - T characteristics of a device, with film thickness 270nm, at various constant frequencies. It is observed that the rate at which the capacitance initially increases with temperature reduces as the applied frequency is increased, and at 1MHz the capacitance shows only a marginal change with increase in temperature. The saturation value of capacitance attained near 250K is approximated as geometric bulk capacitance, C_b, as that obtained at liquid nitrogen temperature. Hence a plot of C_b versus inverse thickness should yield a straight line. Fig. 7 shows the C_b versus 1/S plot, which is a straight line. The dielectric constant calculated using the slope of the curve is found to be 12 which is in agreement with the values reported for other similar material [11].

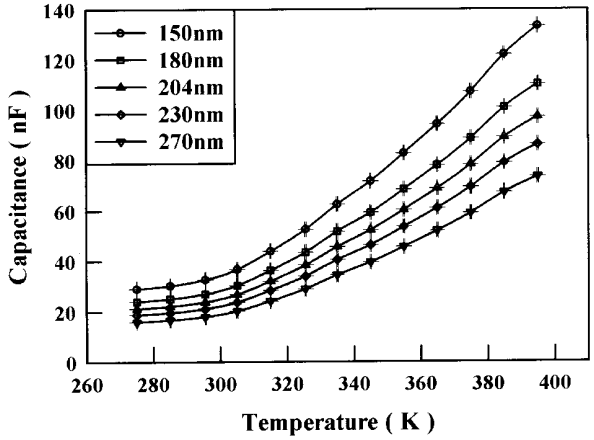

Figure 5. Capacitance versus temperature characteristics of the devices with different film thicknesses and at fixed applied frequency, 1KHz.

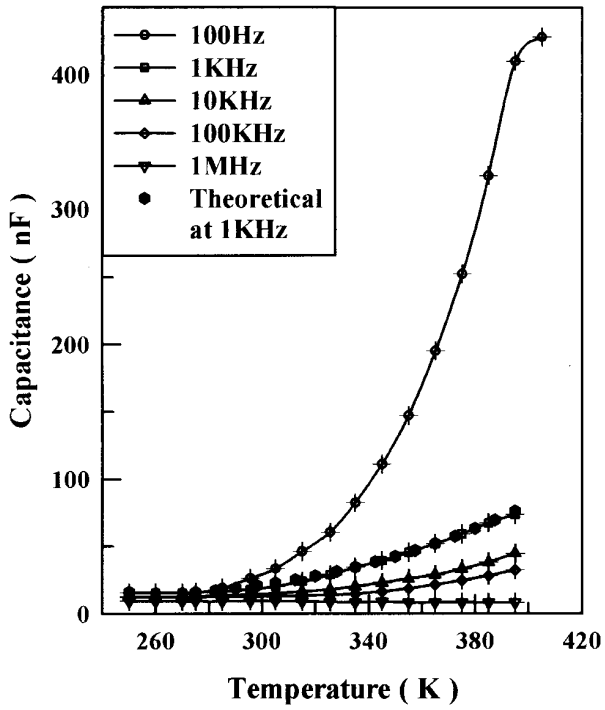

Figure 6. Capacitance versus temperature characteristics of the device with film thickness 270nm for different frequencies.

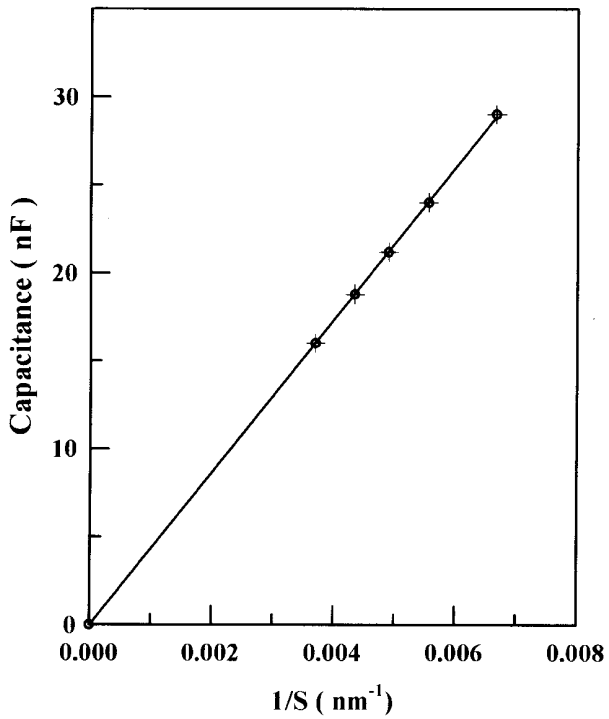

Figure 7. Capacitance versus inverse film thickness plot at 250K.

Fig. 8 shows the temperature variation of tan $\delta - \omega$ characteristics of a typical representative device with film thickness 270nm. It is seen that the dielectric loss initially decreases with the increase in frequency, attains a minimum, and then starts increasing monotonically. The frequency, at which tan δ attains minimum, $\omega_{\min}$, is found to increase with increase in device temperature.

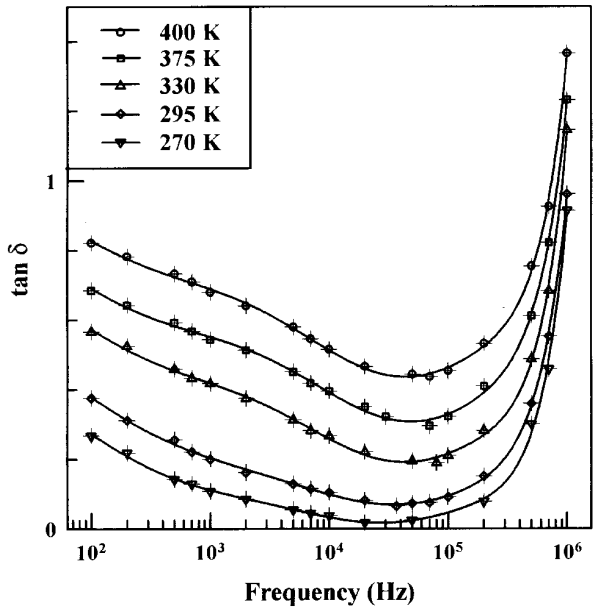

Figure 8. Tan δ versus frequency characteristics of the device with film thickness 270nm at different temperatures.

IV Discussion

The ac characteristics are usually explained on the basis of either of the three models, namely, Debye relaxation model [12,13], Schottky barriers model [14,15] or growth of aluminium oxide at the metal-insulator interface [16].

However, for Debye relaxation process the low frequency to the high frequency capacitance ratio is expected typically to be 3:1 [13] while the observed ratio in case of our films is 12:1. Further, the Debye relaxation model is based on polarization of a material and applicable to a few polar solids [17]. As reported [10], the X-ray diffractograph of the evaporated $Sb_2Pb_1Se_7$ film shows sharp peaks corresponding only to PbSe and Se_6. It is known that PbSe is very strong bond [18] while Se_6 is hexagonal in structure. Hence both, PbSe and Se_6 cannot be readily polarized. This implies that, in the present case, the evaporated material is non-polar in nature and hence the observed dielectric properties of the samples cannot be explained on the basis of Debye relaxation model.

In the case of Schottky barriers model the ratio of low frequency to high frequency capacitance could be typically 20:1 [14] while the observed ratio is 12:1. It has also been observed during the low field dc measurements [19], that the dc conduction is governed by space charge limited conduction mechanism which demands the electrode contacts to be ohmic. Also all the dc characteristic curves were identical in nature even if the polarity of the electrodes was reversed. Thus the observed ac characteristics can not be explained on the basis of Schottky barriers model also.

The third possibility is the growth of oxide at the aluminium material interfaces. The growth of such oxide can be made easily evident from the C-T characteristics where the decrease in the magnitude of the capacitance is observed in each heating and cooling cycle [16]. However, no such phenomenon was observed and the C-T curve traced identical path during heating and cooling of the sample. This is also to be expected, as the entire deposition sequence was completed without braking vacuum at any stage. Thus allowing the interfaces to get exposed to the oxygen in air.

Thus it is evident that the observed characteristics cannot be explained on the basis of these models. An attempt is therefore, made to interpret the observed characteristics using a basic small signal ac circuit analysis [20].

As shown in Fig. 9(a), the measured capacitance can be represented as a bulk capacitance, C_b, in parallel with the bulk resistance, R_b both in series with the lead resistance $r/2$ on either side. The effective parallel and series impedances of this circuit can be given by,

$$Z_p = r + (C_b ll R_b) \qquad (1)$$

and

$$Z_s = R_s + \frac{1}{j\omega C_s}. \tag{2}$$

With

$$R_s = r + \frac{R_b}{1+\omega^2 C_b^2 R_b^2} \tag{3}$$

and

$$C_s = \frac{1+\omega^2 C_b^2 R_b^2}{\omega^2 C_b R_b^2} = \frac{1}{\omega^2 C_b R_b^2} + C_b \equiv a + b \tag{4}$$

$$R_b = R_0 \exp\left(\frac{\Delta E}{kT}\right) \tag{5}$$

where

R_b = Bulk resistance
C_h = Bulk capacitance
$r/2$ = Lead resistance
R_o = Characteristic resistance of bulk material
R_s = Effective series resistance
C_s = Effective series capacitance
T = Temperature
ΔE = Activation energy of carriers

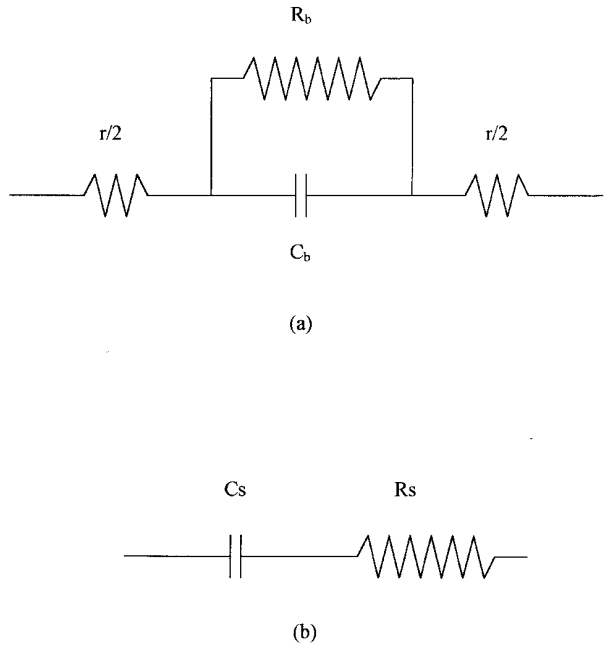

Figure 9. (a) General representation; (b) Equivalent series circuit.

Thus the equivalent circuit shown in Fig. 9(a) can be represented as shown in the Fig. 9(b). The above equations and the equivalent circuit shown in the Fig. 9(b) will be used for the analysis of the results. The desired parameters are chosen in the following manner. It is seen from equation 4 that when the applied signal frequency is very high the measured capacitance approaches the bulk capacitance value. Hence the high frequency capacitance, i.e., in the present case, capacitance at 1MHz, can be approximated as the bulk capacitance of the material for any given thickness. Thus the bulk capacitance of the material for the thickness 270nm is 10nF. Also ΔE is chosen as 0.09eV and R_0 as 393Ω.

IV.1 Variation of capacitance with temperature

With the help of the above parameters the theoretical values of the capacitance were computed for various temperature, for the representative sample with film thickness 270nm. The theoretical C - T curve calculated for frequency 1KHz is shown by hexagon in Fig. 6. It is seen that there is excellent agreement between experimental and theoretical curves.

Differentiating capacitance with temperature,

$$\frac{dC_s}{dT} = \frac{da}{dT} = \frac{2\Delta E}{\omega^2 C_b R_b^2 k T^2} > 0 \tag{6}$$

Since, all the terms on the right hand side are positive; capacitance is an increasing function of temperature. In the above equation, right hand side term is inversely proportional on square of the applied frequency. This implies that the rate of change of capacitance, i.e., slope of C - T plot decreases as the temperature of the device increases (ref. Fig. 6). Temperature coefficient of capacitance (TCC) can be given by,

$$TCC = \frac{dC_s}{dT} \times \frac{1}{C_s} \tag{7}$$

Since, all the terms in the above equation are positive, TCC is an increasing function of temperature. This is shown in the Fig. 10.

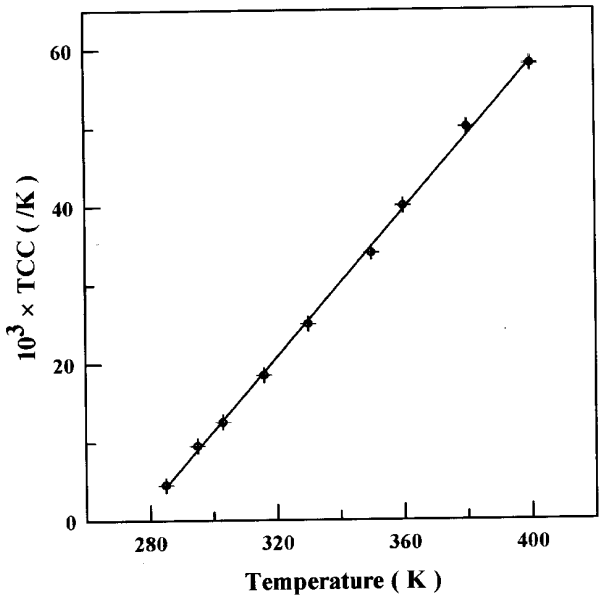

Figure 10. TCC versus temperature characteristics of the device with film thickness 270nm for 1 KHz frequency.

IV.II Variation of tan δ with frequency

Dielectric loss, tan δ, in general, can be given by,

$$\tan\delta = \omega C_s R_s \tag{8}$$

Substituting for C_s and R_s, the equation 8 may be written as,

$$\tan\delta = \omega \times \frac{1+\omega^2 C_b^2 R_b^2}{\omega^2 C_b R_b^2} \times \left(r + \frac{R_b}{1+\omega^2 C_b^2 R_b^2}\right) \tag{9}$$

Differentiating tan δ with respect to ω, we get,

$$\frac{d(\tan\delta)}{d\omega} = -\left(\frac{1}{\omega^2 C_b R_b}\right) - \left(\frac{1}{\omega^2 C_b R_b^2}\right) + rC_b \tag{10}$$

And second differentiation will be

$$\frac{d^2\tan\delta)}{d\omega^2} = \frac{2}{\omega^3 C_b R_b} + \frac{2r}{\omega^3 C_b R_b^2} > 0 \tag{11}$$

Since all the terms in the above equation are positive, tan δ must go through a minimum value at a critical frequency, $\omega_{\min}$. Hence equation 10 must be zero at critical frequency, $\omega_{\min}$. Thus,

$$-\left(\frac{1}{\omega_{\min}^2 C_b R_b}\right) - \left(\frac{r}{\omega_{\min}^2 C_b R_b^2}\right) + rC_b = 0 \tag{12}$$

Since lead resistance, $r/2$, is very small compared to the bulk resistance, R_b, of the material, the second term in the above equation approaches zero. Hence neglecting this term, the above equation may be written as,

$$\omega_{\min} = -\left(\frac{1}{rC_b^2 R_b}\right)^{1/2} \tag{13}$$

Equation 13 shows that the critical frequency $\omega_{\min}$ depends on the bulk resistance, which is temperature dependent such that R_b decreases as temperature increases (refer equation 5). Hence, $\omega_{\min}$ should depend on temperature such that $\omega_{\min}$ should increase as temperature increase, which is precisely what is observed (refer Fig. 8).

V Conclusion

The $Sb_2Pb_1Se_7$7 films are prepared by vacuum deposition of the compound. The observed capacitance and dielectric loss as a function of frequency and temperature can be satisfactorily explained on the basis of small signal ac circuit analysis. The theoretical curve generated using the analysis show excellent fitting with corresponding experimental curve.

References

[1] S. Prakash, S. Ashokan, J. Phys. D **29**(7), 2004 (1996).

[2] W.J. Bresser, J. Wells, M. Zhang, P. Boolchand, Z. Nat-forsch. A Phys. Phys. Chem. Kosmophys (Germony) A **51**(5-6), 373 (1996).

[3] S.J. Lade, M.D. Ulpane, M.M. Ulpane, C.D. Lokhande, J. Mater. Sci. **9**, 477 (1999).

[4] E. Sagbo, D. Houphouet-Boigny, R. Eholic, J.C. Jumas, J. Olivier-Fourcadu, M. Mouriu, J. Rivet, J. Solid State Chemistry (USA), **113**, 145 (1994).

[5] A.A. Simashkevich, S.D. Shutov, Semicond. (USA), **28**, 80 (1994).

[6] A. Vidourek, L. Tichy, M. Vlcek, Mater. Lett. (Nether), **22**(12), 59 (1995).

[7] J.C. Giuntini, S.S. Soulayman, Zanchetta, Apply. Phys. A. Mater. Sci. Process (Germony), A **60**, 309 (1995).

[8] A. Daoudi, J.C. Levet, M. Potel, H. Noel, MaterRes. Bull. (USA), **31**(10), 1213 (1996).

[9] L.I. Maissel and R. Glang, *Handbook of thin film Technology*, McGraw Hill book Company, (1970).

[10] S. Wagle, V. Shirodkar, Czeck. J. Phys. **50**, 635 (2000).

[11] G.S. Nadkarni, N. Sankarraman and S. Radhakrishnan, J. Phy. D: Apply. Phys. **16**, 897 (1983).

[12] A. Kumar, K.N. Laxminarayanan, K.K. Srivastava, Ind. J. Pure and Apply. Physics **18**, 318 (1980).

[13] O.S. Panwar, M. Radhakrishana, K.K. Srivastava, Philos. Mag. B **41**(3), 253 (1980).

[14] G.S. Nadkarni, J.G. Simmons, J. Apply. Physics **43**, 3741 (1972).

[15] G.S. Nadkarni, V.S. Shirodkar and J.G. Simmons, Thin Solid Films **94**, 101 (1982).

[16] S. Radhakrishna, Ph.D. Thesis, University of Mumbai.

[17] C.P. Smyth, *Dielectric Behaviour and Structure*, McGraw Hill Book Company Inc. (1955)

[18] D.R. Lide, *Handbook of Chemistry and Physics*, McGraw Hill book company, 76th edition (1995-96).

[19] S. Wagle and V. Shirodkar, Brazilian J. Phys. **30**, In press (2000).

[20] P. Cutler and H. Hoover, *Electronic Circuit Analysis* (Passive networks) Vol. 1 (1960).